

Polyamidoamine Dendronized Hollow Fiber Membranes in the Recovery of Heavy Metal Ions

Qian Zhang,[†] Na Wang,[†] Libo Zhao,[†] Tongwen Xu,^{*,†} and Yiyun Cheng^{‡,*,§}

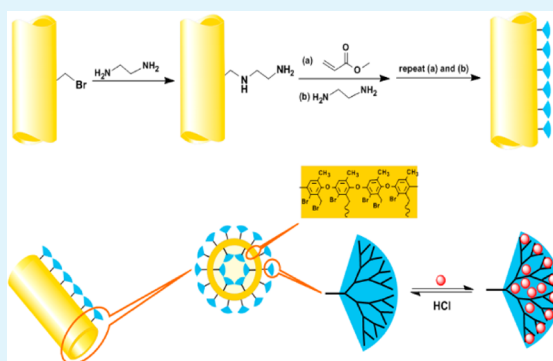
[‡]Shanghai Key Laboratory of Regulatory Biology, School of Life Sciences, [§]Shanghai Key Laboratory of Magnetic Resonance, Department of Physics, East China Normal University, Shanghai, 200062, People's Republic of China

[†]CAS Key Laboratory of Soft Matter Chemistry, Department of Chemistry, University of Science and Technology of China, Hefei, Anhui, 230026, People's Republic of China

Supporting Information

ABSTRACT: Polyamidoamine (PAMAM) dendronized hollow fiber membranes (HFMs) were synthesized and used in the recovery of heavy metal ions. The dendronized HFMs showed strong binding ability with Cu^{2+} , Pb^{2+} , and Cd^{2+} ions. Generation 3 (G3) PAMAM dendronized HFM (G3-HFM) retained 72% of its Cu^{2+} binding capacity after five cycles of use and recovery. Interestingly, $\text{Cu}_2(\text{OH})_3\text{Cl}$, $\text{Pb}_3(\text{CO}_3)_2(\text{OH})_2$, and CdCO_3 crystals were grown on G3-HFM surface when G3-HFMs were immersed in CuCl_2 , $\text{Pb}(\text{NO}_3)_2$, and CdCl_2 solutions, respectively, while no crystal was observed with nonmodified HFMs. The results provide new insights into the applications of membrane-supported dendrimers in the recovery of heavy metal ions.

KEYWORDS: dendrimer, dendron, PAMAM, hollow fiber membrane, nanocrystal, heavy metal ion



INTRODUCTION

Dendrimers are a class of hyperbranched macromolecules with a tree-like architecture. They possess well-defined ellipsoidal or globular structures with precisely defined molecular weight and number of surface functionality especially at low generations.^{1–3} These features make dendrimers hot research points in miscellaneous fields including supramolecular chemistry, host–guest chemistry, noble metal nanoparticle synthesis, catalysts, pollution removal, and biomedical applications.^{4–11} Among the reported dendrimers, poly(amidoamine) (PAMAM) dendrimers synthesized by Tomalia in 1985 are one of the most success dendrimer families.¹² PAMAM dendrimers are soluble in a variety of solvents and were intensively characterized by different techniques.¹³ They can be easily functionalized both on the surface and in their interior.^{2,14–18} PAMAM dendrimers and their derivatives are now commercially available from Dendritech or NanoSynthons Inc. Although high cost is involved with these promising polymers, recently developed click chemistry allows the synthesis of high-generation PAMAM dendrimers within a couple of days,¹⁹ which will significantly reduce the schedule and cost during dendrimer synthesis.

PAMAM dendrimers have well-defined numbers of tertiary amine ($2^{n+2}-2$ for ethylenediamine (EDA)-cored PAMAM dendrimer, n is dendrimer generation) and primary amine (2^{n+2}) groups in the interior and on the surface, respectively. Also, there are a large number of amide groups ($2^{n+2}-4$) in the PAMAM dendrimer pockets. These groups have a high capacity

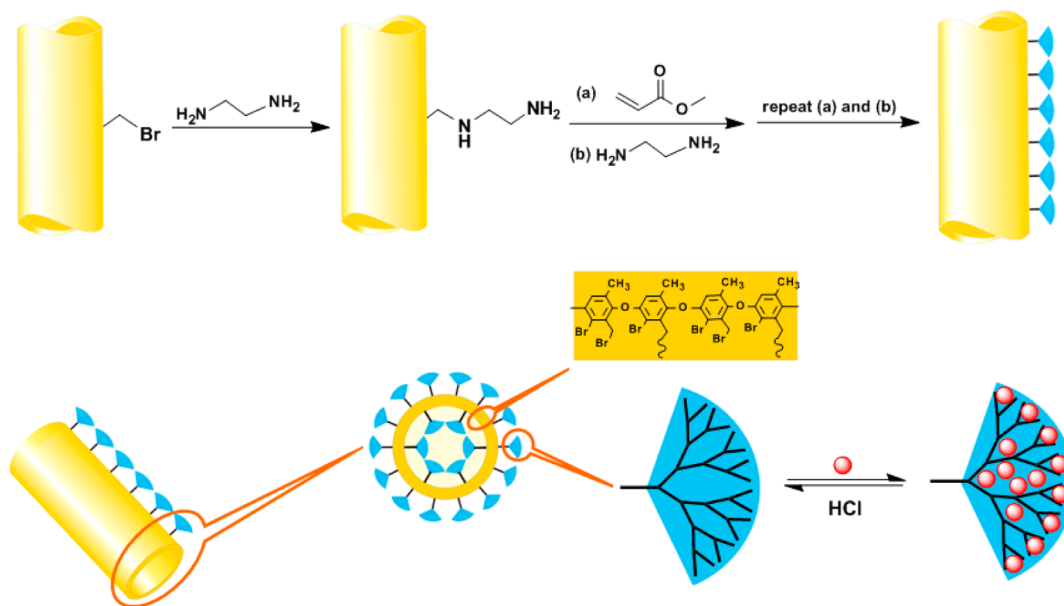
to bind heavy metal ions through coordination bonds.^{20–26} The first studies of dendrimer and metal ion complexation focused on Cu^{2+} .²⁷ Generation 2, 3, and 6 hydroxyl-terminated PAMAM dendrimers were reported to bind 4, 8, and 64 Cu^{2+} ions in aqueous solutions, respectively. The number of bound Cu^{2+} ions is in linear relationship with the number of interior tertiary amine groups.²¹ Besides Cu^{2+} ions, the complexation of Pb^{2+} , Cd^{2+} , Fe^{3+} , Ni^{2+} , Pt^{2+} , Ag^+ , Au^{3+} , Pd^{3+} , Mn^{2+} , Ru^{3+} , and U^{6+} with PAMAM dendrimers were reported.^{21,26,28} The dendrimer and metal ion complexes can act as precursors to prepare dendrimer encapsulated nanoparticles by reducing the bound metal ions.^{4,20,22,25} In addition, strong binding affinity of these heavy metal ions with PAMAM dendrimers indicates their applications in the extraction of heavy metal ions from water.^{26,27,29–31} The bound metal ions can be released by protonation of the primary and tertiary amine groups on dendrimer scaffold, which means the dendrimers can be recovered after metal ion complexation. Diallo et al. reported the recovery of Cu^{2+} from aqueous solutions using a PAMAM dendrimer enhanced ultrafiltration technology.²⁹ Zhao et al. further explored the potential application of PAMAM dendrimers in the removal of Cu^{2+} and Pb^{2+} from contaminated soils.^{30,31} Though high percent of spent PAMAM dendrimers can be recovered through nano-

Received: January 14, 2013

Accepted: March 7, 2013

Published: March 7, 2013

Scheme 1. Synthetic Route of PAMAM Dendronized HFMs and Their Applications in the Recovery of Heavy Metal Ions from Water



filtration, the high cost of cellulose membranes and nanofilters as well as the operation cost should be considered. Also, the nanofiltration membranes are easily fouled by the environmental pollutions and the retained dendrimers. These reasons prevent the practical applications of PAMAM dendrimers in the removal of heavy metal ions from water.

Solid material-supported dendrimers are efficient alternatives in the removal of metal ions from water. The material-supported dendrimers can be easily recovered by taking the materials out of water and the dendrimers can be recovered by washing them with acidic water. In previous studies, solid materials such as carbon nanotubes,³² mesoporous silica,³³ and Fe₃O₄ magnetic nanoparticles³⁴ were functionalized with PAMAM dendrimers for catalysis, protein immobilization, and biomedical applications. Here, we prepared PAMAM dendronized hollow fiber membranes by grafting PAMAM dendrons from bromomethylated poly(2,6-dimethyl-1,4-phenylene oxide) (BPPO) hollow fiber membranes (HFMs).³⁵ BPPO is a versatile polymer that was widely used in the preparation of ion-exchange membranes.³⁶ They are chemically stable, nondegradable materials in traditional solvents, and can be easily fabricated into HFMs and functionalized for various purposes.³⁷ The versatile properties of BPPO and PAMAM dendrimer make PAMAM dendronized BPPO a promising material in the extraction of metal ions. As shown in Scheme 1, the bromide groups on BPPO were functionalized with amine groups and the amines were further reacted with methyl acrylate and ethylenediamine to synthesize PAMAM dendrons as described elsewhere.^{3,35}

RESULTS AND DISCUSSION

Figure 1 shows the effect of PAMAM dendron generation on the adsorption of heavy metal ions (Cu²⁺, Pb²⁺, Cd²⁺) by PAMAM dendronized HFMs in aqueous solutions. The surface color of G1-G5 BPPO HFMs turned from light yellow to green after Cu²⁺ binding, while that of nonmodified BPPO HFM is scarcely changed, suggesting the binding of large amounts of Cu²⁺ on the surface of dendronized HFMs (see Figure S1 in the

Supporting Information). Higher-generation PAMAM dendronized HFMs show higher binding affinity toward the three metal ions. G3-HFM exhibits the highest binding ability toward the three metal ions. Surprisingly, the metal ion loading abilities of G4- and G5-HFMs are lower than that of G3-HFMs. Take Cu²⁺ for example, the Cu²⁺ ion binding capacity of G3-HFMs is 37.37 mg/g, while the values for G4- and G5-HFMs are 26.09 and 25.42 mg/g, respectively. From macroscopic observation, partial surfaces of the G4- and G5-HFMs were stripped from the membranes, which is probably due to the decreased mechanical strengths of high generation PAMAM dendronized HFMs. In scanning electron microscopy (SEM) studies, we observed that the surface of G1-, G2-, and G3-HFMs is smooth, whereas that of G4- and G5-HFMs are relatively rough (see Figure S2 in the Supporting Information). Stripped surfaces of the HFMs means decreased PAMAM dendron densities on the HFMs. As a result, G4- and G5-HFMs showed lower metal ion binding capacity than G3-HFM. The highest ion binding ability of G3-HFM is also observed when PAMAM dendronized HFMs were used in the adsorption and release of ionic drugs such as sodium methotrexate, Congo red, and sodium salicylate.³⁵

Among the three metal ions, G3-HFM shows the higher binding capacity toward Cu²⁺ ion (583.8 μmol Cu²⁺/g dry G3 HFM) than toward Pb²⁺ and Cd²⁺ ions (263.6 μmol Pb²⁺/g and 255.6 μmol Cd²⁺/g dry G3 HFM, respectively). This is probably due to the higher binding affinity of PAMAM dendrimers with Cu²⁺ ions than with Pb²⁺ and Cd²⁺ ions.^{30,31} The bound metal ions by G1-G5 HFMs are scarcely desorbed in deionized water. To regenerate the PAMAM dendronized HFMs, the metal ion bound G1-G5 HFMs were treated with HCl (pH 2) and washed with deionized water. After HCl treatment, the surfaces of Cu²⁺ bound G1-G5 BPPO HFMs turn back to light yellow, indicating the desorption of Cu²⁺ ions from PAMAM dendrons on the surface of HFMs (see Figure S1 in the Supporting Information). About 80, 76, and 78% of the bound Cu²⁺, Pb²⁺, and Cd²⁺ ions were desorbed from G3-HFM, respectively (Figure 1). As shown in the SEM images of G3-HFM cross sections (see Figure S3 in the Supporting

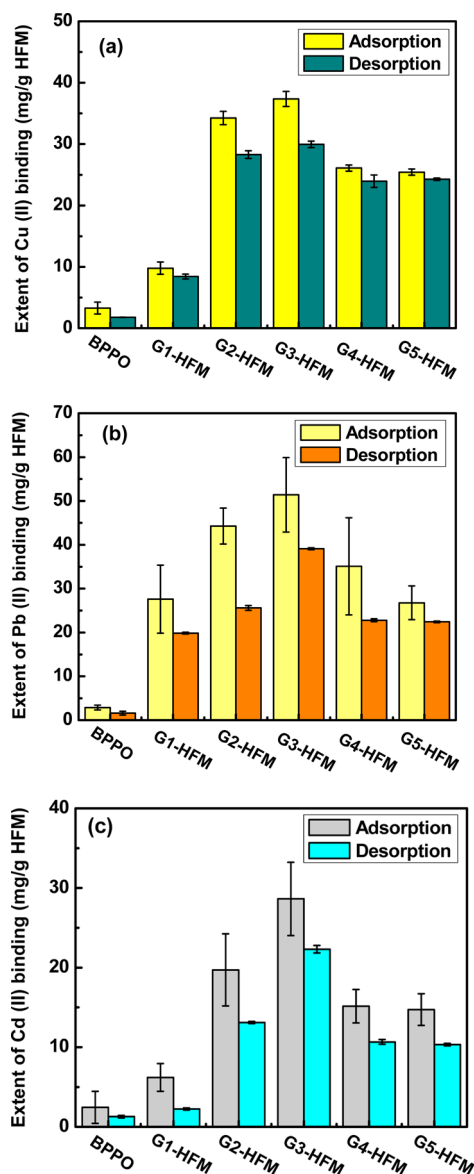


Figure 1. Adsorption and desorption of metal ions by G1-G5 HFMs and nonmodified BPPO HFM. (a) Cu^{2+} , (b) Pb^{2+} , and (c) Cd^{2+} .

Information), finger-shaped macrovoids with a diameter of 5–10 μm and large numbers of holes with a size round 500 nm were observed. These cavities within BPPO HFMs are functionalized with a high density of PAMAM dendrons. There are several steps for an interior-bound metal ion to escape from the dendronized HFMs: (1) release of metal ion from its original binding site at acidic conditions, (2) diffusion of the metal ion from HFM interior to its surface through the finger-shape macrovoids and the nanoscale holes, (3) recapture and release of the metal ion by PAMAM dendrons on the walls of macrovoids and holes. The PAMAM dendrons will significantly retard the diffusion of released Cu^{2+} out of the HFMs. In addition, the amide groups within the interior pockets of PAMAM dendrons can bind metal ions at acidic conditions (pH 2). As a result, there are still around 20% of the metal ions bound by PAMAM dendrons modified on G3-HFM in the desorption studies.

Traditional chelating agents such as ethylenediaminetetraacetic acid (EDTA), nitrilotriacetic acid (NTA), and pyridine-

2,6-dicarboxylic acid (PDA) were widely used to bind heavy metal ions. However, excess chelating agent and bound metal ions are difficult to be recovered from the wastewater.³⁰ PAMAM dendrimers have nanoscale size, globular shape, and high chelating ability with heavy metal ions.^{27,29} The metal ion-bound dendrimer can be recovered by nanofiltration through a commercial available cellulose membrane.²⁹ The advantage of using dendronized BPPO HFMs for the removal of heavy metal ions in this study is that we do not need cellulose membrane and nanofiltration process to recover the spent dendrimers. In a previous study using PAMAM dendrimers to bind Cu^{2+} ions, approximately 60%–72% of the spent PAMAM dendrimers can be recovered by incubation of dendrimer/ Cu^{2+} complexes with 2 N HCl solutions after one cycle of use and recovery.³⁰ In comparison, G3-HFM in the current study can restore 72.0% of its binding affinity with Cu^{2+} after five cycles of use and recovery (see Figure S4 in the Supporting Information), whereas the values for Pb^{2+} and Cd^{2+} ions are 90.6 and 68.8%, respectively. It is worth noting that the residual 20% metal ions remained within HFM can be released by using a 2 M HCl solution as described in the references, we considered the part of unreleased metal ions in each cycle when calculating the binding capacity of dendronized HFM. PAMAM dendronized HFMs are not soluble in water as well as other organic solvents. This property enables the recovery of dendrimers and metal ions by simple separation process. These results suggest that PAMAM dendronized BPPO HFMs may serve as reusable materials for the recovery of heavy metal ions from wastewater.

The surface morphology of PAMAM dendronized HFMs after adsorption of the three metal ions were characterized by SEM analysis. Surprisingly, nanocrystals were observed on the surfaces of Cu^{2+} , Pb^{2+} , and Cd^{2+} treated G3-HFMs. As shown in Figure 2, polydispersed crystals (needlelike, plateletlike, cuboid-shaped, and irregularly shaped) are observed on the surface of Cu^{2+} -treated G3-HFM. In comparison, plateletlike crystals were observed on the surface of Pb^{2+} -treated G3-HFM, and the nanostructures observed on the surface of Cd^{2+} -treated G3-HFM exhibited a cubic morphology and consisted of dozens of nanocrystals. Both outer and inner surfaces of the G3-HFMs are observed with crystals and no crystal is observed in the fingerlike macrovoids of the HFMs. Because the metal-ion-bound G3-HFM was washed with deionized water for three times before drying, the observed crystals should not be due to physically adsorbed metal salts such as $\text{CuCl}_2 \cdot 2\text{H}_2\text{O}$, $\text{Pb}(\text{NO}_3)_2$, and $\text{CdCl}_2 \cdot 2.5\text{H}_2\text{O}$. In addition, no crystals were observed on the surface of Cu^{2+} , Pb^{2+} , and Cd^{2+} treated nonmodified BPPO HFMs (see Figure S5 in the Supporting Information), suggesting that PAMAM dendrons on the surface of HFMs play an important role in the growth of the crystals.

The elements and compositions of the crystals grown on the surface of G3-HFMs were further analyzed by energy dispersive X-ray spectroscopy (EDX) and X-ray powder diffraction (XRD) (see Figure S6 in the Supporting Information and Figure 3). The EDX results are collected from the crystal area in the SEM images. As shown in Figure S6 in the Supporting Information, the EDX spectrum of crystals on the surface of Cu^{2+} treated G3-HFM shows strong peaks for Cu, Cl, and O elements. Similarly, the EDX spectra of Pb^{2+} - and Cd^{2+} -treated samples show Pb, C, O and Cd, C, O peaks, respectively. Au peaks are observed in the EDX spectra in Figure S6 in the Supporting Information because of the gold coating deposited on the samples before SEM experiments. The EDX results suggest that Cu, Pb, and Cd are confirmed as componential

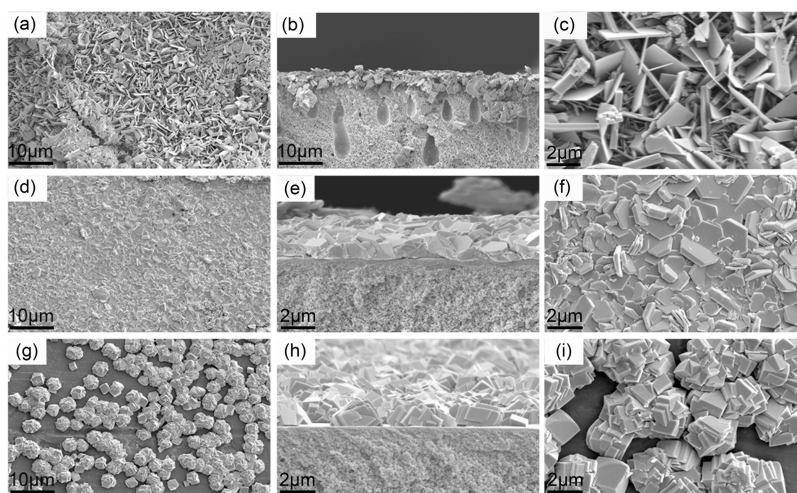


Figure 2. SEM images of G3-HFM (a, c, d, f, g, i) surface and (b, e, h) cross-section after metal ion adsorption. (a–c) Cu^{2+} , (d–f) Pb^{2+} , and (g–i) Cd^{2+} .

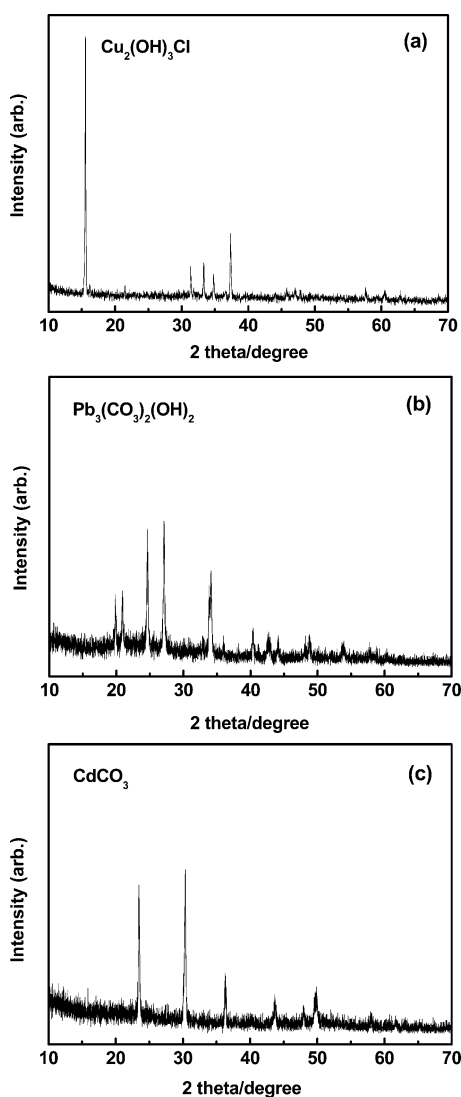
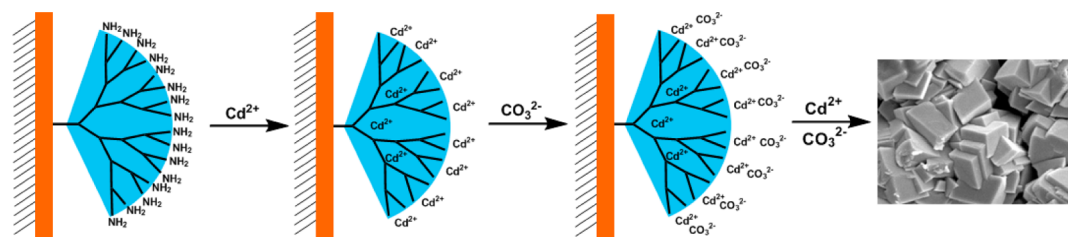


Figure 3. XRD spectra of the crystals grown on the surface of metal ion treated G3-HFMs. (a) Cu^{2+} , (b) Pb^{2+} , and (c) Cd^{2+} . The JCPDS card numbers of pure $\text{Cu}_2(\text{OH})_3\text{Cl}$, $\text{Pb}_3(\text{CO}_3)_2(\text{OH})_2$, and CdCO_3 are 85–1713, 12–0131, and 42–1342, respectively.

elements in the three crystals, respectively. The EDX spectra of the three metal ion treated BPPO HFMs only show C, O, and Br peaks, which are the compositions of nonmodified BPPO (see Figure S7 in the Supporting Information). The crystal compositions are analyzed to be $\text{Cu}_2(\text{OH})_3\text{Cl}$, $\text{Pb}_3(\text{CO}_3)_2(\text{OH})_2$, and CdCO_3 , respectively from the XRD spectra in Figure 3. One may assume that the $\text{Pb}_3(\text{CO}_3)_2(\text{OH})_2$ and CdCO_3 crystals are formed during the HFM drying process. To exclude this possibility, we also dried the metal ion-bound G3-HFMs by vacuum lyophilization and no carbon dioxide should participate in the formation of $\text{Pb}_3(\text{CO}_3)_2(\text{OH})_2$ and CdCO_3 crystals during this process. The crystals treated by lyophilization were then characterized by SEM and XRD. As shown in Figures S8 and S9 in the Supporting Information, neither the crystal morphology nor the crystal composition and structure are changed. Therefore, the crystals should be formed during the adsorption experiments in the aqueous solutions. The crystal growth is probably initiated by the complexation of metal ions with PAMAM dendrons on HFM surface, followed by the adsorption of $\text{CO}_3^{2-}(\text{OH}^-)$ ions to the complexed metal ions and/or the primary amine groups on the surface of PAMAM dendrons. After that, more metal ions and $\text{CO}_3^{2-}(\text{OH}^-)$ ions are bound to the PAMAM dendron/metal ion complexes and in situ growth of $\text{Pb}_3(\text{CO}_3)_2(\text{OH})_2$ and CdCO_3 crystals took place on the surface of dendronized HFMs (Scheme 2). The CO_3^{2-} ions possibly come from the dissolved CO_2 in the metal ion solutions. The CdCO_3 crystal growth on G3-HFM is similar to biomineralization of CdCO_3 crystals on the bacteria membrane.³⁸ The PAMAM dendron/metal ion complexes on the HFM surface may act as the nucleation center during crystal growth.

In previous reports on the extraction of heavy metal ions using dendrimers, the binding mechanisms of metal ions by PAMAM dendrimers were proposed to be: (1) complexation with surface primary amine groups, (2) complexation with interior tertiary amine and amide groups, and (3) physical encapsulation within dendrimer interior cavities or interactions with trapped counterions or water molecules.^{21,29,30,39} However, in the case of dendrimer-modified porous materials such as dendronized HFMs, we find that the formation of metal salt crystals on the material surface also plays an important role in the binding and extraction of heavy metal ions from water.

Scheme 2. Mechanisms of CdCO₃ Crystal Growth on the Surface of PAMAM Dendronized HFMs

Recently, Han et al. prepared hyperbranched PAMAM/polysulfone composite membranes for the removal of Cd²⁺ ions from water.⁴⁰ Hyperbranched PAMAM used as chelating agents was incorporated into polysulfone via a phase inversion process. PAMAM and polysulfone were complexed together via electrostatic interactions in their composites. They did not observe the crystal growth of CdCO₃ inside or on the surface of their ion-absorbing membranes. This is probably due to the high density of PAMAM dendrons grown on the surface of BPPO HFM in this study. It is the first report on the growth of metal salt crystals on the surface of dendrimer functionalized solid materials. This interesting phenomenon provides new insights into the extraction of heavy metal ions from wastewater and the applications of solid material-supported dendrimers.

CONCLUSION

We investigated the heavy metal ion binding ability of PAMAM dendronized HFMs. G3-HFM exhibits the highest loading capacity toward Cu²⁺, Pb²⁺, and Cd²⁺. Cu²⁺ has a higher binding affinity with G3-HFM than Pb²⁺ and Cd²⁺. G3-HFM can retain about 70% of its metal ion loading capacity after five cycles of use and recovery. An interesting phenomenon on the metal ion bound G3-HFMs is the growth of Cu₂(OH)₃Cl, Pb₃(CO₃)₂(OH)₂, and CdCO₃ crystals on the surface of G3-HFMs during the metal ion adsorption process. The growth of metal ion containing crystals on the surface is one of the metal ion loading mechanisms of dendronized HFMs. Further crystal growth mechanism on the surface of PAMAM dendronized HFMs is still under investigation and we are currently evaluating the in situ growth of hydroxyapatite crystals on PAMAM dendronized HFMs for the repair of bone defects.

ASSOCIATED CONTENT

Supporting Information

Further information on Experimental Section, SEM images, and XRD data of the crystals grown on the surface of dendronized HFMs. This material is available free of charge via the Internet at <http://pubs.acs.org>.

AUTHOR INFORMATION

Corresponding Author

*E-mail: twxu@ustc.edu.cn (T.X.); yycheng@mail.ustc.edu.cn (Y.C.).

Notes

The authors declare no competing financial interest.

ACKNOWLEDGMENTS

The authors greatly acknowledge the financial supports from the Science and Technology of Shanghai Municipality (11DZ2260300), the Talent Program of East China Normal

University (77202201), and the National Natural Science Foundation of China (21025626) on this project.

REFERENCES

- (1) Tomalia, D. A. *Soft Matter* **2010**, *6*, 456–474.
- (2) Tomalia, D. A. *New J. Chem.* **2012**, *36*, 264–281.
- (3) Tomalia, D. A. *Prog. Polym. Sci.* **2005**, *30*, 294–324.
- (4) Astruc, D.; Boisselier, E.; Ornelas, C. *Chem. Rev.* **2010**, *110*, 1857–1959.
- (5) Astruc, D.; Ornelas, C.; Ruiz, J. *Acc. Chem. Res.* **2008**, *41*, 841–856.
- (6) Cheng, Y. Y.; Zhao, L. B.; Li, Y. W.; Xu, T. W. *Chem. Soc. Rev.* **2011**, *40*, 2673–2703.
- (7) Hu, J. J.; Xu, T. W.; Cheng, Y. Y. *Chem. Rev.* **2012**, *112*, 3856–3891.
- (8) Caminade, A. M.; Ouali, A.; Keller, M.; Majoral, J. P. *Chem. Soc. Rev.* **2012**, *41*, 4113–4125.
- (9) Caminade, A. M.; Majoral, J. P. *Chem. Soc. Rev.* **2010**, *39*, 2034–2047.
- (10) Caminade, A. M.; Majoral, J. P. *Acc. Chem. Res.* **2004**, *37*, 341–348.
- (11) Zhao, L. B.; Wu, Q. L.; Cheng, Y. Y.; Zhang, J. H.; Wu, J. H.; Xu, T. W. *J. Am. Chem. Soc.* **2010**, *132*, 13182–13184.
- (12) Tomalia, D. A.; Baker, H.; Dewald, J.; Hall, M. G. K.; Martin, S.; Roeck, J.; Ryder, J.; Smith, P. *Polym. J.* **1985**, *17*, 117–132.
- (13) Caminade, A. M.; Laurent, R.; Majoral, J. P. *Adv. Drug Delivery Rev.* **2005**, *57*, 2130–2146.
- (14) Hu, J. J.; Su, Y. Z.; Zhang, H. F.; Xu, T. W.; Cheng, Y. Y. *Biomaterials* **2011**, *32*, 9950–9959.
- (15) Wang, Y.; Guo, R.; Cao, X.; Shen, M.; Shi, X. Y. *Biomaterials* **2011**, *32*, 3322–3329.
- (16) Shi, X. Y.; Lee, I. H.; Chen, X. S.; Shen, M. W.; Xiao, S. L.; Zhu, M. F.; Baker, J. R., Jr.; Wang, S. H. *Soft Matter* **2010**, *6*, 2539–2545.
- (17) Shi, X. Y.; Wang, S. H.; Van Antwerp, M. E.; Chen, X.; Baker, J. R., Jr. *Analyst* **2009**, *134*, 1373–1379.
- (18) Shi, X. Y.; Sun, K.; Baker, J. R., Jr. *J. Phys. Chem. C* **2009**, *112*, 8251–8258.
- (19) Killops, K.; Campos, L. M.; Hawker, C. J. *J. Am. Chem. Soc.* **2008**, *130*, 5062–5064.
- (20) Yancey, D. F.; Carino, E. V.; Crooks, R. M. *J. Am. Chem. Soc.* **2010**, *132*, 10988–10989.
- (21) Crooks, R. M.; Zhao, M. Q.; Sun, L.; Chechik, V.; Yeung, L. K. *Acc. Chem. Res.* **2001**, *34*, 181–190.
- (22) Gomez, M. V.; Guerra, J.; Velders, A. H.; Crooks, R. M. *J. Am. Chem. Soc.* **2009**, *131*, 341–350.
- (23) Gomez, M. V.; Guerra, J.; Myers, V. S.; Crooks, R. M.; Velders, A. H. *J. Am. Chem. Soc.* **2009**, *131*, 14634–14635.
- (24) Carino, E. V.; Crooks, R. M. *Langmuir* **2011**, *27*, 4227–4235.
- (25) Balogh, L.; Tomalia, D. A. *J. Am. Chem. Soc.* **1998**, *120*, 7355–7356.
- (26) Diallo, M. S.; Arasho, W.; Johnson, J. H., Jr.; Goddard, W. A. *Environ. Sci. Technol.* **2008**, *42*, 1572–1579.
- (27) Diallo, M. S.; Balogh, L.; Shafagati, A.; Johnson, J. H., Jr.; Goddard, W. A., III; Tomalia, D. A. *Environ. Sci. Technol.* **1999**, *33*, 820–824.
- (28) Liu, Y. H.; Crooks, R. M. *C. R. Chimie* **2003**, *6*, 1049–1059.

- (29) Diallo, M. S.; Christie, S.; Swaminathan, P.; Johnson, J. H., Jr.; Goddard, W. A., III *Environ. Sci. Technol.* **2005**, *39*, 1366–1377.
- (30) Xu, Y. H.; Zhao, D. Y. *Environ. Sci. Technol.* **2005**, *39*, 2369–2375.
- (31) Xu, Y. H.; Zhao, D. Y. *Ind. Eng. Chem. Res.* **2006**, *45*, 1758–1765.
- (32) Campidelli, S.; Sooambar, C.; Diz, E. L.; Ehli, C.; Guldi, D. M.; Prato, M. *J. Am. Chem. Soc.* **2006**, *128*, 12544–12552.
- (33) Jiang, Y. J.; Gao, Q. *J. Am. Chem. Soc.* **2005**, *128*, 716–717.
- (34) Pan, B. F.; Gao, F.; Gu, H. C. *J. Colloid Interface Sci.* **2005**, *284*, 1–6.
- (35) Zhang, Q.; Wang, N.; Xu, T. W.; Cheng, Y. Y. *Acta Biomater.* **2012**, *8*, 1316–1322.
- (36) Wang, N.; Wu, C. M.; Wu, Y. H.; Xu, T. W. *J. Membr. Sci.* **2010**, *363*, 128–139.
- (37) Wang, N.; Wu, C. M.; Cheng, Y. Y.; Xu, T. W. *Int. J. Pharm.* **2011**, *408*, 39–49.
- (38) Diels, L.; van Roy, S.; Taghavi, S.; van Houdt, R. *Antonie van Leeuwenhoek* **2009**, *96*, 247–258.
- (39) Diallo, M. S.; Christie, S.; Swaminathan, P.; Balogh, L.; Shi, X. Y.; Um, W.; Papelis, C.; Goddard, W. A., III; Johnson, J. H., Jr. *Langmuir* **2004**, *20*, 2640–2651.
- (40) Han, N. K.; Yu, B. Y.; Kwak, S. Y. *J. Membr. Sci.* **2012**, *396*, 83–91.